SensCAP: A Systematic Sensing Capability Performance Metric for 6G ISAC

Guangyi Liu, Liang Ma, Yahui Xue, Lincong Han, Rongyan Xi, Zixiang Han, *Member, IEEE*, Hanning Wang, Jing Dong, Mengting Lou, Jing Jin, Qixing Wang, and Yifei Yuan, *Fellow, IEEE*

***Abstract*—The sixth generation mobile communication system (6G) will provide everything as a service (XaaS), where X includes communication, sensing, computing, artificial intelligence (AI), big data and security, and more. Novel features, such as Sensing as a Service (SaaS), will contribute to further realizing Internet of Everything (IoE). Integrated sensing and communication (ISAC) is identified as one of the six usage scenarios for 6G by the international telecommunication union radiocommunication sector (ITU-R), and the corresponding studies on the detailed technical performance requirements and evaluation methodologies have begun in 2024. Although ISAC has become a popular topic, there are no systematic performance requirements metrics and corresponding evaluation methodologies defined for SaaS in a mobile communication system, while conventional key performance indicators (KPIs) for radar systems have been borrowed currently. Therefore, to fill this gap, this article proposes SensCAP, a systematic capability performance metric composed of sensing capacity, accuracy, and probability. The sensing capacity reflects the comprehensive sensing performance, which can be expressed as the number of targets that can be detected per unit area within unit time, given sensing Quality-of-Service (QoS) requirements consisting of sensing accuracy and probability. Furthermore, the performance evaluation of the SensCAP is conducted through system simulation using proposed evaluation methodologies, and the KPI values are suggested as the guidelines for further study in ITU-R.**

***Index Terms*—Evaluation methodologies, integrated sensing and communication (ISAC), international telecommunication union radiocommunication sector (ITU-R), Quality of Service (QoS), sixth generation (6G), standardization, technical performance requirements, test environments.**

I. Introduction

THE-SIXTH-GENERATION (6G) mobile communication network will provide a variety of services by embracing enhanced communication and novel capabilities, including sensing, computing, artificial intelligence (AI), big data, and security. These novel capabilities are native-designed and implemented to achieve Internet of Everything (IoE) [1], [2], [3], which is the paradigm shift for 6G. Novel capabilities, such as sensing and AI, will transform mobile network operators from communication-service providers to information-service providers, and realize the vision of digital twin and ubiquitous intelligence [4], [5], [6]. Integrated sensing and communication (ISAC) is one of the major emerging technologies for 6G, and the key use cases include intelligent transportation, such as vehicle-to-everything (V2X) and unmanned aerial vehicle (UAV) economy, as well as smart manufacturing [7], [8], as shown in Fig. 1. From the technical perspective, sensing and communication have similar data processing flow in terms of signal generation, transmission, reception and processing. Moreover, communication systems are evolving to higher frequencies and larger antenna arrays, which is *de facto* for radar sensing systems. Thus, the integration of sensing and communication is an inevitable trend [9]. Different levels of integration will lead to various folds of benefits, for example, hardware-level integration will lead to cost reduction, signal-level integration will save the spectrum and bring performance enhancement, and data-level integration will cultivate new applications [10], [11], [12].

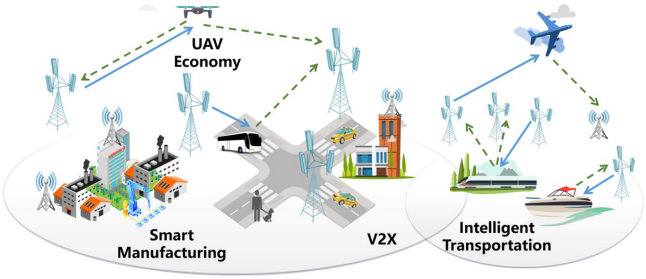

Fig. 1. Typical use cases of ISAC.

The 6G standardization has entered a new phase. In June 2023, international telecommunication union radiocommunication sector (ITU-R) working party 5D (WP 5D) finished the international mobile telecommunications-2030 (IMT-2030) Framework Recommendation [13] after a two-and-a-half-year study. This milestone document has defined 6G vision and identified six usage scenarios and 15 key capabilities for 6G. IMT-2030 Framework Recommendation has revealed guidelines and design principles for 6G, with enhanced as well as novel scenarios and capabilities, including ISAC. As shown in Fig. 2, from 2024 to 2026, ITU-R WP 5D will investigate technical performance requirements, evaluation methodologies, test environments and evaluation criteria for IMT-2030 (6G), laying the foundations for technology proposal evaluation which will take place later from 2028 to 2029 [14]. Similar reports have been published for previous generations, for example, [15] is the technical performance

Manuscript received 1 April 2024; revised 26 June 2024 and 10 July 2024; accepted 11 July 2024. Date of publication 18 July 2024; date of current version 6 September 2024. *(Corresponding author: Liang Ma.)*

The authors are with the Future Research Lab, China Mobile Research Institute, Beijing 100053, China (e-mail: maliangyjy@chinamobile.com).

Digital Object Identifier 10.1109/JIOT.2024.3430502

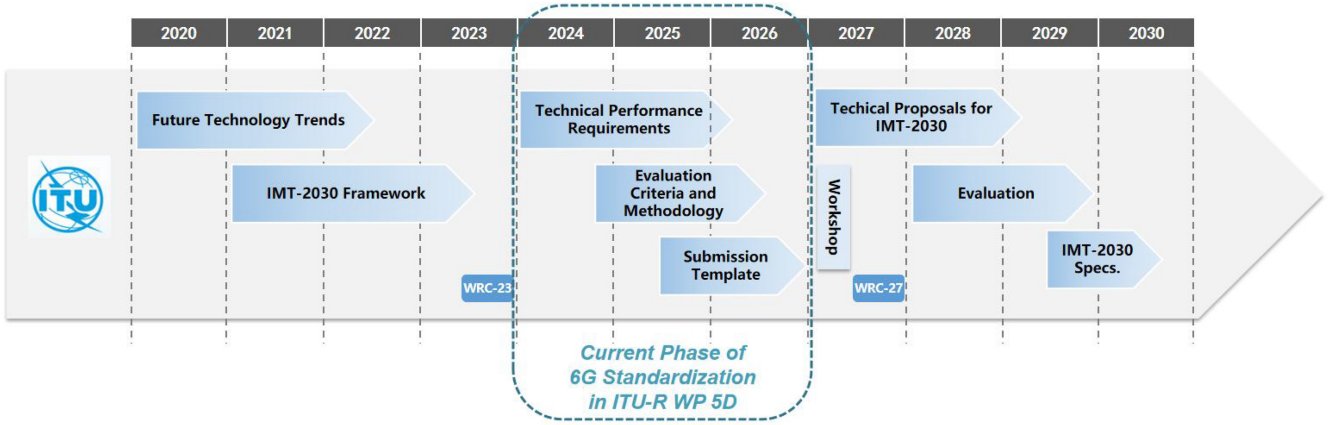

Fig. 2. ITU-R IMT-2030 timeline.

requirements and [16] is the evaluation methodology for IMT-2020 (5G). Therefore, the technical performance requirements, evaluation methodologies and test environments of new IMT-2030 capabilities, such as sensing, are vital for the next phase of 6G research and standardization.

There are several key components required to define and evaluate the performance of Sensing as a Service (SaaS), including technical performance requirement definition, evaluation methodology, test environment, simulation platform and configuration, and ISAC channel modeling. Research on certain topics has already begun, but with more work to be done. In terms of key performance indicator (KPI) definition, Third Generation Partnership Project (3GPP) Service and System Aspects Working Group 1 (SA1) has finished the feasibility study on ISAC [17], 32 use cases and their performance requirements have been defined. However, the KPIs defined are mostly conventional radar system requirements, such as accuracy of positioning estimate, sensing resolution, refreshing rate, etc. Besides, these KPIs are not technical performance requirements but are rather drawn from service demands. Regarding the 32 use cases identified, a down-selection focusing on the essential ones is needed to define suitable test environments for evaluation.

In terms of ISAC channel modeling, 3GPP Radio Access Network Working Group 1 (RAN1) has initiated the study on the ISAC channel model since 2024 [18], [19]. The channel modeling should be based on measurements and simulation, and a number of related studies have been conducted [20], [21], [22], [23], [24]. In addition, the channel correlation between communication and sensing is an essential topic to discuss, relevant research includes [25], [26], [27], [28] and more. The 3GPP ISAC channel modeling study is still in progress and will pave the way for evaluation methodologies once it is finished.

Regarding evaluation methodology, simulation platform and configuration, little work has been completed. The ISAC system simulation is the simulation for the entire system of both sensing and communication, which encompasses system-level simulation and link-level simulation. Although system-level and link-level sensing simulations can be borrowed from those of communication, the unified ISAC system simulation is still absent.

Therefore, this article intends to fill the gap in the field of KPI definition, evaluation methodology, test environment, simulation platform and configuration. To the best of the author's knowledge, currently, there is no publication detailing technical performance requirements and evaluation methodologies for sensing capabilities. Therefore, the main contribution of this article is to propose a systematic technical performance requirement metric for sensing capabilities, as well as corresponding evaluation methodologies and test environments. For the first time, we propose SensCAP, a systematic capability performance metric composed of sensing capacity, sensing accuracy, and sensing probability, and their corresponding evaluation methodologies. SensCAP reflects the comprehensive sensing performance, namely, the number of targets, that can be detected per unit area within unit time, given sensing Quality-of-Service (QoS) requirements which consist of sensing accuracy and probability. The suggested KPI values of SensCAP are given based on ISAC system simulations.

The remainder of this article is organized as follows and is illustrated in Fig. 3: Section II introduces the definition of SensCAP. Section III gives the evaluation methodologies for SensCAP. Section IV presents the system model and sensing processing algorithm which is used for evaluation. Section V introduces the test environments, network layouts, simulation parameters and the novel unified ISAC system simulation platform. Section VI shows simulation results and analysis. Section VII concludes this article by providing SensCAP KPI values and suggesting future research directions.

II. SensCAP—Defining Technical Performance Requirements for Sensing Capabilities

In this section, we give the definition of SensCAP which is a systematic capability performance metric consisting of sensing capacity, accuracy, and probability. We first introduce sensing probability, which indicates the ability to detect the presence of targets and is the prerequisite for accurate sensing. Then we discuss sensing accuracy which shows the individual sensing performance of certain targets. Sensing probability and sensing accuracy build up sensing QoS. Sensing capacity is then defined as the number of targets that can be detected

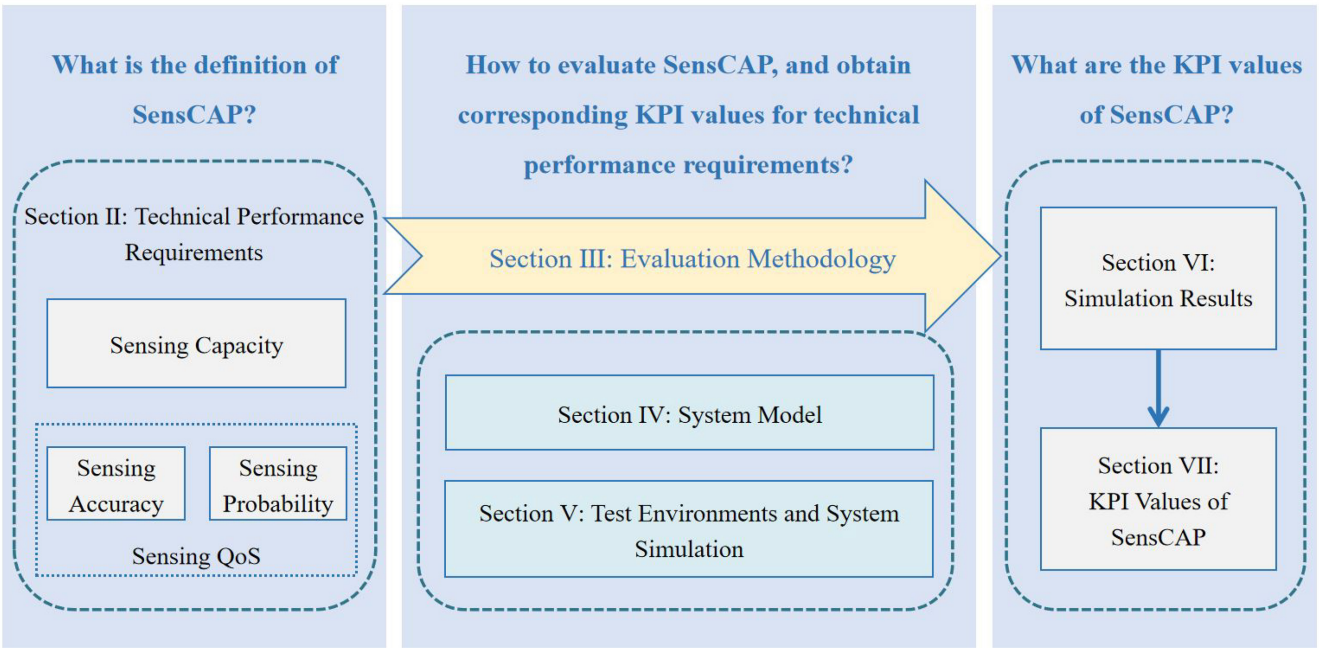

Fig. 3. Main contributions and core structure of this article.

given sensing QoS, which reflects the comprehensive sensing performance.

A. Sensing Probability

1) Definition: Detection probability and false alarm rate are typical radar requirements. For the sensing probability defined here, we focus on the detection probability for a given false alarm rate. The sensing probability is defined as the ratio of successfully detected targets to the total number of targets, with a given false alarm rate as the prerequisite for obtaining the detection probability. Sensing probability shows the ability to detect the presence of sensing targets (STs), which is inherent in high-performance sensing.

The reason for defining sensing probability as above is two fold. First, the typical values of false alarm rate are smaller than 10^{-6} [29], which is difficult to evaluate through simulations as the target sample size is not large enough in ISAC evaluation setups. Second, using the false alarm rate as the input to acquire detection probability is the proper evaluation approach, more discussions are shown below.

2) Relationship Between Detection Probability and False Alarm Rate: In this section, we demonstrate the relationship between the detection probability and the false alarm rate to further elaborate on sensing probability. When detecting the presence of a target, one of the following two assumptions must hold:

$$\begin{cases} \mathcal{H}_0 : \mathbf{y} = \mathbf{w} \\ \mathcal{H}_1 : \mathbf{y} = \mathbf{s} + \mathbf{w} \end{cases} \tag{1}$$

where the first assumption indicates that there is only noise and the second assumption indicates that there is noise and the target, and $\mathbf{y}$ denotes the observation vector based on N sample data. The probability capacity function (PDF) describes the observations that need to be tested based on any of the

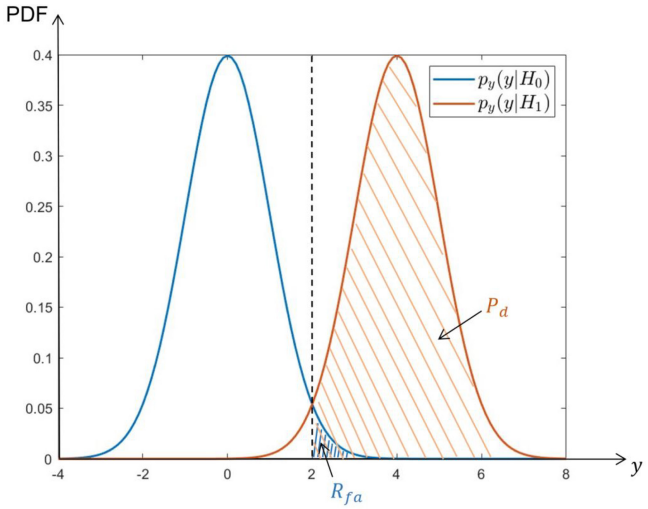

Fig. 4. PDFs under $\mathcal{H}_0$ and $\mathcal{H}_1$ assumptions.

hypothetical cases. The $p_{\mathbf{y}}(\mathbf{y}|\mathcal{H}_1)$ and $p_{\mathbf{y}}(\mathbf{y}|\mathcal{H}_0)$ are the PDFs of the observation vector for the presence and absence of the target, respectively. Detection probability P_d means a target is detected in the presence of a target, and false alarm rate R_{fa} means that a target is detected in the absence of a target. For example, as shown in Fig. 4, the two PDFs denote $p_{\mathbf{y}}(\mathbf{y}|\mathcal{H}_0)$ and $p_{\mathbf{y}}(\mathbf{y}|\mathcal{H}_1)$, where the P_d and R_{fa} are expressed as the area of the two PDFs from the threshold of black line to $+\infty$, respectively.

In the field of radar sensing, the Neyman–Pearson criterion is usually used for target detection [30]. Such criterion indicates the detection performance is optimized while ensuring that the false alarm rate does not exceed the tolerable range, i.e.,

$$\max P_d, \ \text{s.t.} \ R_{fa} \leq \alpha \tag{2}$$

where α is the maximum false alarm rate. This optimization problem can be solved by the method of Lagrange multipliers as follows:

$$F = P_d + \lambda\big(R_{fa} - \alpha\big). \tag{3}$$

To find the optimal solution to maximize F, the following expressions can be obtained:

$$\frac{p_{\mathbf{y}}(\mathbf{y}|\mathcal{H}_1)}{p_{\mathbf{y}}(\mathbf{y}|\mathcal{H}_0)} \underset{H_0}{\overset{H_1}{\gtrless}} -\lambda \tag{4}$$

where λ is a detection threshold. The decision criteria represent the likelihood ratio test [31]. The presence or absence of the target depends on the observation $\mathbf{y}$ and the detection threshold λ. Therefore, we define the sensing probability as the detection probability for a given false alarm rate.

3) Detection Algorithm: For radar sensing systems, one of the most commonly used detection algorithms is the constant false alarm rate (CFAR) detection algorithm. The CFAR detector adaptively determines the detection threshold while maintaining a certain number of false alarms [32]. When target detection is performed on the received signal, since the noise power of different detection units usually changes, the noise power of each detection unit needs to be estimated. Hence, in CFAR detection, we first obtain noise power by calculating the average power of the adjacent units, which is effectively the noise power of the current detection unit. Next, we choose a false alarm rate R_{fa} that meets the demand, and then calculate the detection threshold of the current detection unit according to the R_{fa} and noise power. Finally, we decide whether there is a target in the current detection unit based on the detection threshold. The detailed mathematical relationship equation is as follows:

$$S_{\text{thres}} = N_{ru} \times \left(R_{fa}^{-\frac{1}{N}} - 1\right) \times p_n \tag{5}$$

where S_{thres} is the detection threshold, N_{ru} denotes the number of reference units used to estimate the noise power, p_n denotes the noise power estimated from N_{ru} reference units, and R_{fa} denotes the given false alarm rate. From (5) we can see that the false alarm rate is a prerequisite for obtaining the detection probability, and vice versa.

B. Sensing Accuracy

1) Definition: Regarding sensing accuracy, we focus on localization accuracy and velocity accuracy. The former can be derived from range estimation and angle estimation, and the latter can be obtained from Doppler estimation. The definition of localization/velocity accuracy is the difference between the estimated localization/velocity and true values. Such performance requirements can be presented as localization accuracy of l_a m for a given confidence level (@ confidence level), and velocity accuracy v_a m/s @ confidence level, where the sensing accuracy can be obtained from the cumulative distribution function (CDF) plot of sensing estimation error given a typical confidence level of 90%. The expression of accuracy @ confidence level is commonly used in the performance evaluation, such as in 3GPP new radio (NR) positioning [33]. The confidence level of 90% means the 90th percentile point on the CDF plot of sensing estimation error, and the corresponding sensing estimation error at 90th percentile point is the value of sensing accuracy.

Moreover, it should be noted that velocity is a vector with direction and magnitude. Thus, at least two receivers are involved when estimating velocity using Doppler information. Another approach using only one receiver for velocity estimation is to calculate average velocity using the location difference of two time-instances divided by the elapsed time. Such a method will reduce certain sensing processing complexities at the cost of nonreal-time results, and the aggregated error introduced by localization estimation may degrade the performance. Detailed sensing localization and velocity estimation algorithms will be presented in Section IV-B.

2) Cramér–Rao Lower Bound: As a lower bound for the mean square estimation (MSE) of any unbiased estimator, Cramér–Rao lower bound (CRLB) is an important tool for the performance evaluation of various estimation methods. Thus, CRLB can demonstrate the theoretical limit of sensing accuracy. Suppose that there are N parameters related to the target to be estimated from the received signal $\mathbf{y}$, such as the target's position, velocity, orientation, etc. They form a parameter vector denoted as $\boldsymbol{\eta} \in \mathbb{C}^{N\times 1}$. Assuming that $\hat{\boldsymbol{\eta}}$ is the unbiased estimator of $\boldsymbol{\eta}$, then the MSE can be lower bounded by the CRLB

$$\mathbb{E}_{\boldsymbol{Y}|\boldsymbol{\eta}}\Big[\big(\hat{\boldsymbol{\eta}} - \boldsymbol{\eta}\big)\big(\hat{\boldsymbol{\eta}} - \boldsymbol{\eta}\big)^T\Big] \succeq \mathbf{J}_{\boldsymbol{\eta}}^{-1} \tag{6}$$

where $\mathbb{E}_{\boldsymbol{Y}|\boldsymbol{\eta}}[\,\cdot\,]$ denotes the conditional expectation operation. The matrix $\mathbf{J}_{\boldsymbol{\eta}}$ is the $N \times N$ fisher information matrix (FIM), with elements [34]

$$\big[\mathbf{J}_{\boldsymbol{\eta}}\big]_{i,j} = \mathbb{E}_{\mathbf{y}|\boldsymbol{\eta}}\left[-\frac{\partial \log f_{\mathbf{y}|\boldsymbol{\eta}}(\mathbf{y}|\boldsymbol{\eta})}{\partial[\boldsymbol{\eta}]_i}\frac{\partial \log f_{\mathbf{y}|\boldsymbol{\eta}}(\mathbf{y}|\boldsymbol{\eta})}{\partial[\boldsymbol{\eta}]_j}\right] \tag{7}$$

where $f_{\mathbf{y}|\boldsymbol{\eta}}(\mathbf{y}|\boldsymbol{\eta})$ denotes the conditional likelihood function of $\mathbf{y}$ under the condition of known $\boldsymbol{\eta}$.

In some cases, the position of the target is estimated through a series of intermediate parameters like channel parameters, containing delay, Angle of Arrival (AoA) and Angle of Departure (AoD), etc., denoted as $\boldsymbol{\zeta}$. Therefore, the FIM of position estimation will be derived from the FIM of channel estimation [35]

$$\mathbf{J}_{\boldsymbol{\eta}} = \mathbf{T}^T\mathbf{J}_{\boldsymbol{\zeta}}\mathbf{T} = \left(\frac{\partial \boldsymbol{\zeta}}{\partial \boldsymbol{\eta}}\right)^T \mathbf{J}_{\boldsymbol{\zeta}}\left(\frac{\partial \boldsymbol{\zeta}}{\partial \boldsymbol{\eta}}\right) \tag{8}$$

where $\mathbf{T}$ is the Jacobian matrix representing the derivation function of $\boldsymbol{\zeta}$ w.r.t. $\boldsymbol{\eta}$. The closed-form expression of sensing accuracy CRLB is not the focus of this article, and the detailed derivation procedures of it can be easily found in a number of publications, such as [36], [37], and [38].

C. Sensing Capacity

The sensing probability and sensing accuracy form sensing QoS, which indicates the sensing service quality that users will experience. Working from sensing QoS, we define sensing capacity, a systematic sensing performance indicator, to demonstrate the comprehensive capabilities of the ISAC system. The definition of sensing capacity is the number

of STs that can be detected per unit area within the unit time, given certain sensing QoS requirements (@sensing QoS) which include sensing accuracy and sensing probability. In other words, sensing capacity indicates that ISAC system can detect N STs per km^2 @localization accuracy of l_a m @velocity accuracy v_a m/s @detection probability of P_d @false alarm rate of R_{fa} within 1 s.

The sensing resource restraint of 1 s (per unit time) is required in order to demonstrate the overall performance of ISAC systems, for both sensing and communication functionalities. However, sensing resource restraint is not rigorous. Although it is not strictly limited, the simulation configurations should include sensing signal duration as an indication of sensing resources used. SensCAP requirements should be met within the sensing signal duration which should be less than 1 s. Furthermore, the ratio of sensing signal duration to unit time 1 s can be perceived as sensing resource utilization. As the total time-frequency-space resources available are limited, hence the tradeoff between communication and sensing performances exists. The sensing resource utilization should be relatively low such that outstanding sensing performances can be achieved without compromising communication.

Sensing capacity is a comprehensive sensing performance requirement, with the consideration of different aspects of sensing service quality, including sensing probability and sensing accuracy. Moreover, sensing capacity also takes into account communication-signal interference on the STs, and poses requirements on sensing resource utilization. Therefore, SensCAP is able to demonstrate the comprehensive performance of ISAC systems, and can provide guidelines for the definition of sensing technical performance requirements.

III. Evaluation Methodologies for SensCAP

This section gives detailed evaluation methodologies for SensCAP. It should be noted that the evaluation of sensing probability and sensing accuracy are not mandatory, they are used for determining KPI values of sensing QoS. The sensing capacity evaluation given sensing QoS requirements is required for candidate technology evaluation. Furthermore, we propose a generic evaluation methodology for sensing, which is suitable for not only SensCAP but also other sensing metrics. In the evaluation methods, the total number of STs that are involved in the simulation is N, and is expressed as the number of dropped STs in the remaining parts.

A. Evaluation Methodology for Sensing Probability

The evaluation methodology of sensing probability is given in Evaluation Methodology 1. It should be noted that the simulation results of sensing probability can be obtained from Evaluation Methodology 3 for sensing capacity. The evaluation methodology defined here is used to determine the requirements for sensing probability and form sensing QoS.

B. Evaluation Methodology for Sensing Accuracy

The evaluation methodology of sensing accuracy is given in Evaluation Methodology 2. It should be noted that the simulation results of sensing accuracy are used to obtain the requirements for sensing accuracy and form sensing QoS. Besides conducting simulations, sensing accuracy requirements can be obtained from mathematical calculations based on sensing resolution. The sensing accuracy can be perceived as plus and minus half of the resolution, where the localization resolution is $c/2B$, velocity resolution is $\lambda/2T$ (c is the speed of light, B is sensing signal bandwidth, λ is the sensing signal wavelength, and T is the sensing signal duration). Therefore, we can get sensing accuracy of $c/4B$ m and $\lambda/4T$ m/s.

It should be noted that sensing resolution is not defined for sensing performance requirements, the reason is twofold. First, we can drop STs such that the inter-ST distance is larger than the localization resolution, but such ST dropping would lose a certain degree of randomness. Second, we can randomly drop STs, when two targets are too close to meet the resolution requirements, then only one target can be correctly detected, and this will be reflected in the sensing probability. Therefore, in the SensCAP definition, we did not give requirements on sensing resolution, with the considerations mentioned above.

Evaluation Methodology 1 Evaluation Methodology for Sensing Probability

1: Perform unified ISAC system simulation using the evaluation parameters in Tables II and III for ISAC test environments, given false alarm rate R_{fa}.
2: Generate sensing transmit signal, and obtain sensing receive signal. Perform sensing signal processing, and record whether a target is present or not.
3: If necessary, run multiple simulation drops by repeating steps 1 and 2, and record the total number of successfully detected targets N_{dect}.
4: Calculate the detection probability $P_d = N_{dect}/N$ for a given false alarm rate R_{fa}, where N is the total number of dropped STs.

Evaluation Methodology 2 Evaluation Methodology for Sensing Accuracy

1: Perform unified ISAC system simulation using the evaluation parameters in Tables II and III for ISAC test environments with 10 STs dropped per Sensing Transmission Reception Point (SensTRxP).
2: Generate sensing transmit signal, and obtain sensing receive signal. Perform sensing signal processing, and obtain localization estimation error Δr and velocity estimation error Δv for each ST.
3: Plot the CDF curves of Δr and Δv, and derive the localization accuracy l_a m and velocity accuracy v_a m/s from the 90th percentile point of the CDF curves, where 90% is the confidence level of localization accuracy and velocity accuracy.

C. Evaluation Methodology for Sensing Capacity

Having obtained the sensing QoS requirements of sensing probability and sensing accuracy, we give the evaluation methodology for sensing capacity as shown in Evaluation Methodology 3. The term "sensing capacity" can also be

Evaluation Methodology 3 Evaluation Methodology for Sensing Capacity

1: Perform unified ISAC system simulation using the evaluation parameters in Tables II and III for ISAC test environments with a total number of N STs dropped.
2: Generate sensing transmit signal, obtain sensing receive signal, and perform sensing signal processing.
3: Record whether a target is present or not for a given false alarm rate R_{fa}, and calculate the detection probability P_{d_result}, which should be better than sensing probability performance requirements P_d.
4: Calculate the localization estimation error Δr and velocity estimation error Δv for each ST detected. Plot the CDF curves of Δr and Δv, derive the percentage $R\%$ that fulfils both localization accuracy QoS requirement of l_a m and velocity accuracy QoS requirement of v_a m/s.
5: If necessary, update N which is the number of dropped STs, and repeat steps 1 and 4 until at least 90% of the targets fulfil sensing QoS requirements (i.e., $R\% \geq 90\%$).
6: Calculate the sensing capacity as $C = N/A$, where A is the SensTRxP area.

named "sensing density," and the "capacity evaluation" or "density evaluation" methodologies are not new. For example, [39] gives the evaluation method for Voice over Internet Protocol (VoIP) capacity, [16] gives the evaluation methods for connection density, where the key takeaway from it can be applied here. The sensing capacity can be expressed as N_c STs per km^2 @localization accuracy of l_a m @velocity accuracy v_a m/s @detection probability of P_d @false alarm rate of R_{fa} within unit time. As illustrated in Section II-C, the sensing resource utilization should be reported as the ratio of sensing time duration to the unit time, in order to demonstrate the overall ISAC performance.

D. Generic Evaluation Methodology for Sensing

Having investigated the evaluation methodologies for sensing probability, accuracy and capacity, it can be found that there are similarities among these. The key concept is first to generate sensing transmit signals, and receive signals after channel convolution. Then perform sensing signal processing, and obtain relevant performance metrics. Therefore, we give a generic evaluation methodology for sensing as shown in Evaluation Methodology 4. The proposed generic evaluation methodology is suitable for evaluating the majority of sensing KPIs, and can be used for not only SensCAP but also other sensing metrics.

To elaborate more on the compatibility and generality of the proposed Generic Evaluation Methodology for sensing, here we compare Evaluation Methodology 4 with Evaluation Methodologies 1–3. Regarding Evaluation Methodology 1 for sensing probability, there are a total of four steps, the procedures are similar to the generic evaluation methodology. For Evaluation Methodology 2 of sensing accuracy, three steps are presented, step 3 in the generic evaluation methodology is not implemented as there is no necessity to repeat steps 1 and 2

Evaluation Methodology 4 Generic Evaluation Methodology for Sensing

1: Perform unified ISAC system simulation and initialize evaluation parameters.
2: Generate sensing transmit signal, obtain sensing receive signal, and perform sensing signal processing.
3: If necessary, update evaluation parameters, and repeat steps 1 and 2 until satisfying certain requirements if any.
4: Obtain relevant sensing performance metrics based on the sensing signal processing results.

TABLE I
MAIN PARAMETERS AND CORRESPONDING DESCRIPTIONS

Parameter	Description
I	Number of SensTRxP
N_T	Number of sensing transmit antennas
N_R	Number of sensing receive antennas
J	Number of CommTRxP as well as the associated UE
M_T	Number of communication transmit antennas
L	Number of OFDM symbols
K	Number of subcarriers
$\mathbf{x}$	Transmit signal
$\mathbf{y}$	Receive signal
$\mathbf{w}$	Noise signal
$\mathbf{H}$	Channel state matrix
ρ	Path loss
Ω	Spatial angle consists of elevation and azimuth
θ	Elevation angle
ϕ	Azimuth angle
f_c	Center frequency
T_s	OFDM symbol duration
f_D	Doppler shift
Δf	Subcarrier spacing
d	Propagation distance of the sensing signal
v	Velocity of the sensing target

when evaluating sensing accuracy. In terms of Evaluation Methodology 3 for sensing capacity, a total of six steps are described, where steps 2–4 correspond to step 2 of the generic evaluation methodology. Steps 3 and 4 of the sensing capacity evaluation describe the fulfilment of sensing QoS which could be omitted, as the sensing QoS has already been briefly mentioned in Step 5, thus we provide steps 3 and 4 in the sensing capacity evaluation methodology for clarity and better readability. If we consider steps 2–4 of Evaluation Methodology 3 for sensing capacity as one step, then there are four steps in total, which have the same structure as the generic evaluation methodology.

IV. System Model and Sensing Processing

This section gives the system model which is used in system simulations, and also presents the sensing signal processing algorithm. We use 5G NR with orthogonal frequency-division multiplexing (OFDM) signals as the foundation of the system model and sensing processing. The sensing algorithm described in this section is the basic approach of sensing, where the delay and Doppler information can be extracted based on the differences between receive and transmit signals. Related parameters in this section are shown in Table I.

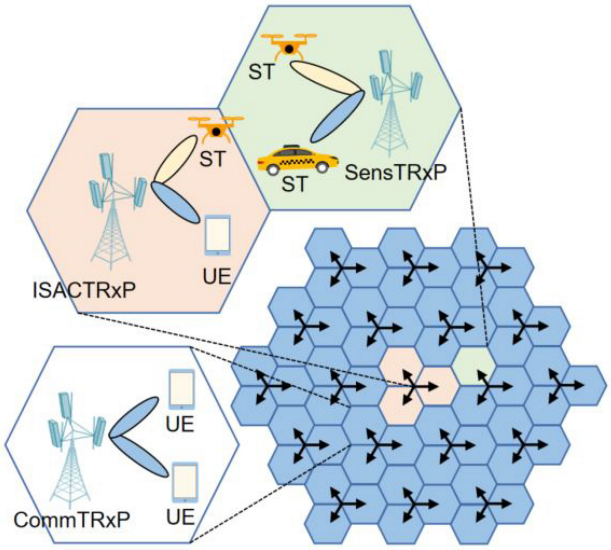

Fig. 5. System model.

A. System Model

As shown in Fig. 5, the ISAC network includes I sensing TRxPs (SensTRxP) with N_T transmitted antennas and N_R received antennas and J downlink communication TRxPs (CommTRxP) with M_T antennas. There are also ISAC TRxPs (ISACTRxP), which can be reduced to a SensTRxP or a CommTRxP for a given period with the assumption of time-duplexed sensing and communication functions. In addition, assume each downlink CommTRxP serves one communication user equipment (UE) in a given OFDM symbol, denoted as UE_j. UEs are equipped with M_R antennas. Such assumption of one UE served per CommTRxP can be easily extended to multiple UEs and we use the current assumption for simplicity.

Regarding sensing process, each SensTRxP_i $(i = 1, \ldots, I)$ transmit sensing reference signals $\mathbf{x}_{s,i} \in \mathbb{C}^{N_T \times 1}$ with the transmission power of $P_{s,i}$. The signal is then reflected by the ST and received by either itself (monostatic) or other SensTRxP (multistatic). The ST could be a connected user or a nonconnected object. This article focuses on device-free sensing where the targets do not participate in sensing signal transmission, reception and processing.

In terms of communication, each CommTRxP_j $(j = 1, \ldots, J)$ transmits communication data signals $\mathbf{x}_{c,j} \in \mathbb{C}^{M_T \times 1}$ with the transmission power of $P_{c,j}$ to UE_j in the serving cell.

For sensing, the signal $\mathbf{y}_{s,i}$ received by SensTRxP_i is presented as follows:

$$\mathbf{y}_{s,i} = \sum_{i'=1}^{I} \left(\mathbf{y}_{s,i,i'} + \mathbf{y}_{ss,i,i'} \right) + \sum_{j=1}^{J} \mathbf{y}_{cs,i,j} + \mathbf{w}_s \tag{9}$$

where $\mathbf{w} \in \mathbb{C}^{N_R \times 1}$ is the noise signal at SensTRxP_i. It should be noted that in the system model defined here, the cluster interference is seen as noise due to its zero-Doppler property. The links between SensTRxPs and STs are Line-of-Sight (LoS). Regarding the non Line-of-Sight (NLoS) sensing, the assumption we made in this work is that NLOS links will lead to much weaker receive signal power, and can be considered as noise. Nevertheless, a variety of studies, such as [40] and [41], focus on NLoS sensing, which will not be thoroughly discussed here.

The sensing signals sent from $\text{SensTRxP}_{i'}$, reflected by ST and received by SensTRxP_i is denoted by

$$\mathbf{y}_{s,i,i'} = \sqrt{\rho_{s,i,i'} P_{s,i'}} \mathbf{H}_{s,i,i'} \mathbf{x}_{s,i'}. \tag{10}$$

And the sensing signals from $\text{SensTRxP}_{i'}$ directly to SensTRxP_i, which contains the self-interference (when $i' = i$) and mutual-interference (when $i' \neq i$), is denoted by

$$\mathbf{y}_{ss,i,i'} = \sqrt{\rho_{ss,i,i'} P_{s,i'}} \mathbf{H}_{ss,i,i'} \mathbf{x}_{s,i'}. \tag{11}$$

Besides, the interference generated by CommTRxP_j on the SensTRxP_i is denoted by

$$\mathbf{y}_{cs,i,j} = \sqrt{\rho_{cs,i,j} P_{c,j}} \mathbf{H}_{cs,i,j} \mathbf{x}_{c,j}. \tag{12}$$

In (10)–(12), $\mathbf{H}_{s,i,i'} \in \mathbb{C}^{N_R \times N_T}$, $\mathbf{H}_{ss,i,i'} \in \mathbb{C}^{N_R \times N_T}$, $\mathbf{H}_{cs,i,j} \in \mathbb{C}^{N_R \times M_T}$, and $\rho_{s,i,i'}$, $\rho_{ss,i,i'}$, $\rho_{cs,i,j}$ are the channel state matrices and path loss for the link from the $\text{SensTRxP}_{i'}$ to the SensTRxP_i reflected by ST, the link from the $\text{SensTRxP}_{i'}$ directly to the SensTRxP_i, and the link from the CommTRxP_j to the SensTRxP_i, respectively. The path loss is presented as follows [42]:

$$\begin{aligned} \rho_{s,i,i'} &= \frac{G_{st} G_{sr} \lambda^2 \sigma_{RCS}}{(4\pi)^3 d_{i,ST}^2 d_{i',ST}^2} \\ \rho_{ss,i,i'} &= \frac{G_{st} G_{sr} \lambda}{(4\pi)^2 d_{i,i'}^2} \\ \rho_{cs,i,j} &= \frac{G_{ct} G_{sr} \lambda}{(4\pi)^2 d_{i,j}^2} \end{aligned} \tag{13}$$

where $d_{i',ST}$, $d_{i,ST}$, $d_{i,i'}$, $d_{i,j}$ are the distances from the $\text{SensTRxP}_{i'}$ to ST, from ST to SensTRxP_i, from $\text{SensTRxP}_{i'}$ to SensTRxP_i, and from CommTRxP_j to SensTRxP_i, respectively. λ is the wavelength, and σ_{RCS} is the radar cross section (RCS) of ST. G_{st}, G_{sr}, G_{ct} are the antenna gains of the SensTRxP's transmitted array, received array and the CommTRxP's transmitted array, respectively.

From (9), we can derive the signal-to-interference-plus-noise ratio (SINR) of the sensing signal received by SensTRxP_i

$$\text{SINR}_{s,i} = \frac{P_{r,s,i}}{\left(I_{c,i} + I_{ss,i} + P_w \right)} \tag{14}$$

where P_w is the noise power, $P_{r,s,i}$ is the received sensing signal power, and $I_{c,i}$ and $I_{ss,i}$ are the interference signal power of the CommTRxPs and SensTRxPs, respectively, on SensTRxP_i

$$\begin{aligned} P_{r,s,i} &= \sum_{i'=1}^{I} \rho_{s,i,i'} P_{s,i'} \left\| \mathbf{H}_{s,i,i'} \right\|_F^2 \\ I_{ss,i} &= \sum_{i'=1}^{I} \rho_{ss,i,i'} P_{s,i'} \left\| \mathbf{H}_{ss,i,i'} \right\|_F^2 \\ I_{c,i} &= \sum_{j=1}^{J} \rho_{cs,i,j} P_{c,j} \left\| \mathbf{H}_{cs,i,j} \right\|_F^2. \end{aligned} \tag{15}$$

For communication, the signal $\mathbf{y}_{c,j}$ received by UE$_j$ is expressed as

$$\mathbf{y}_{c,j} = \sqrt{\rho_{c,j}P_{c,j}}\mathbf{H}_{c,j}\mathbf{x}_{c,j} + \sum_{i=1}^{I}\sqrt{\rho_{sc,j,i}P_{s,i}}\mathbf{H}_{sc,j,i}\mathbf{x}_{s,i} + \sum_{j'=1,j'\neq j}^{J}\sqrt{\rho_{cc,j,j'}P_{c,j'}}\mathbf{H}_{cc,j,j'}\mathbf{x}_{c,j'} + \mathbf{w}_c \quad (16)$$

where the first term of the right-hand side is the data signal from CommTRxP$_j$, the second term is the interference from SensTRxPs, the third term is the interference caused by other CommTRxPs to UE$_j$, and the fourth term is the noise signal at CommTRxP$_j$. $\mathbf{H}_{c,j}, \mathbf{H}_{cc,j,j'} \in \mathbb{C}^{M_R\times M_T}$, $\mathbf{H}_{sc,j,i} \in \mathbb{C}^{M_R\times N_T}$ and $\rho_{c,j}$, $\rho_{cc,j,j'}$, $\rho_{sc,j,i}$ are the channel state matrices and path loss of the link from CommTRxP$_j$ to UE$_j$, from CommTRxP$_{j'}$ to UE$_j$, and from the SensTRxP$_i$ to UE$_j$, respectively. Besides, $\rho_{c,j}$, $\rho_{cc,j,j'}$, $\rho_{sc,j,i}$ has similar expression as $\rho_{cs,i,i'}$.

Based on (16), the SINR of the communication signal received by UE$_j$ is calculated as follows:

$$\mathrm{SINR}_{c,j} = \frac{\rho_{c,j}P_{c,j}\left\|\mathbf{H}_{c,j}\right\|_F^2}{\left(I_{c,j} + I_{s,j} + P_w\right)} \quad (17)$$

where $I_{c,j}$ and $I_{s,j}$ are the power of the interference signals from other CommTRxPs and the SensTRxPs, respectively, on UE$_j$

$$I_{c,j} = \sum_{j'=1,j'\neq j}^{J}\rho_{cc,j,j'}P_{c,j'}\left\|\mathbf{H}_{cc,j,j'}\right\|_F^2$$
$$I_{s,j} = \sum_{i=1}^{I}\rho_{sc,j,i}P_{s,i}\left\|\mathbf{H}_{sc,j,i}\right\|_F^2. \quad (18)$$

B. Sensing Algorithm and Signal Processing

In this section, the location and velocity estimation algorithm is demonstrated for the cooperative sensing systems where multiple monostatic sensing processing is involved, and such an algorithm can be reduced to a single monostatic processing easily. To obtain the expected sensing results, we need to first extract the AoA, signal propagation distance and radial velocity from the received signal of each SensTRxP.

Regarding AoA estimation, we can first compensate the received signal by using the steering vector of the antenna array $\mathbf{a}_i(\Omega)$, $i = 1, 2, \ldots, I$, as

$$g_i(\Omega, k, l) = \mathbf{a}_i^H(\Omega)\mathbf{y}_i(k, l) \quad (19)$$

where I is the total number of SensTRxPs, and $\Omega = (\theta, \phi)$ denotes the spatial angle with θ and ϕ referring to the elevation and azimuth angles in spherical coordinates, respectively. By calculating the sum power received from each angle as

$$h_i(\Omega) = \sum_{l=0}^{L-1}\sum_{k=0}^{K-1}|g_i(\Omega, k, l)|^2 \quad (20)$$

we can obtain $\hat{\Omega}_i = (\hat{\theta}_i, \hat{\phi}_i)$ which is the AoA, including the elevation and azimuth angles of STs, by searching the peaks of $h_i(\Omega)$, where $l = 0, \ldots, L-1$, and $k = 0, \ldots, K-1$ are the OFDM symbol index and subcarrier index of a resource element (RE), with L and K are the total number of OFDM symbols and subcarriers, respectively.

We can then estimate signal propagation distance and radial velocity by the estimated AoA $\hat{\Omega}_i$. Dividing g_i in (19) by the transmit symbols s_i, we have

$$\tilde{g}_i(\Omega, k, l) = \frac{g_i(\Omega, k, l)}{s_i} \quad (21)$$

which is equivalent to the sensing channel information plus noise and interference. Therefore, we can perform 2-D discrete Fourier transform (2D-DFT) on $\tilde{g}_i$ [43] as

$$\tilde{G}_i(p, q) = \frac{1}{kl}\sum_{l=0}^{L}\sum_{k=0}^{i}\tilde{g}_i(\Omega, k, l) \times e^{-j\left(p-\frac{l}{2}\right)\frac{2\pi}{l}l}e^{j(q-1)\frac{2\pi}{i}k}. \quad (22)$$

The phase induced by the time delay τ and radial velocity can be compensated when

$$T_s f_D = \frac{\left(\hat{p}_i - \frac{l}{2}\right)}{l} \quad (23)$$
$$\tau\Delta f = \frac{\left(\hat{q}_i - 1\right)}{k} \quad (24)$$

where $(\hat{p}_i, \hat{q}_i)$ is the peak index of OFDM symbols and subcarrier in $\tilde{g}_i$, f_D is the Doppler offset caused by the radial velocity, Δf is the subcarrier spacing, and T_s is the symbol duration. The propagation distance $\hat{d}_i$ and the radial velocity $\hat{v}_{\parallel,i}$ of sensing objects can then be solved as

$$\hat{v}_{\parallel,n} = \frac{\left(\hat{p}_i - \frac{l}{2}\right)c}{lT_s f_c} \quad (25)$$
$$\hat{d}_i = \frac{(\hat{q}_i - 1)c}{k\Delta f}. \quad (26)$$

Based on the AoA $\hat{\Omega}_i = (\hat{\theta}_i, \hat{\phi}_i)$, propagation distance $\hat{d}_i$ and radial velocity $\hat{v}_{\parallel,n}$ estimated by I SensTRxPs, we can optimize the position estimation of ST as follows. Assuming that the coordinate of SensTRxP$_i$ is (x_i, y_i, z_i) and the coordinate of ST is (x, y, z), we can formulate the optimization problem as

$$(x, y, z) \coloneqq \min_{x,y,z}\sum_{k=1}^{i}\alpha_i\left|\hat{d}_i - 2d_i\right| + \sum_{k=1}^{i}\beta_i\left|\hat{\theta}_i - \theta_i\right| + \sum_{k=1}^{i}\gamma_i\left|\hat{\phi}_i - \phi_i\right| \quad (27)$$

where $d_i = \sqrt{(x-x_i)^2 + (y-y_i)^2 + (z-z_i)^2}$ is the distance between SensTRxP$_i$ and ST, $\theta_i = \arccos([z - z_i]/d_i)$ and $\phi_i = \arctan([y - y_i]/[x - x_i])$ are the elevation and azimuth angle of the ST with respect to SensTRxP$_i$, α_i, β_i, and γ_i are the weighting coefficients for the results estimated by SensTRxP$_i$. The optimization problem (27) can be quickly solved by using the interior-point method with the optimal estimation of ST position being $(\hat{x}, \hat{y}, \hat{z})$ [44].

Next, we estimate object velocity, denoted as (v_x, v_y, v_z), based on the estimated object position $(\hat{x}, \hat{y}, \hat{z})$ and radial

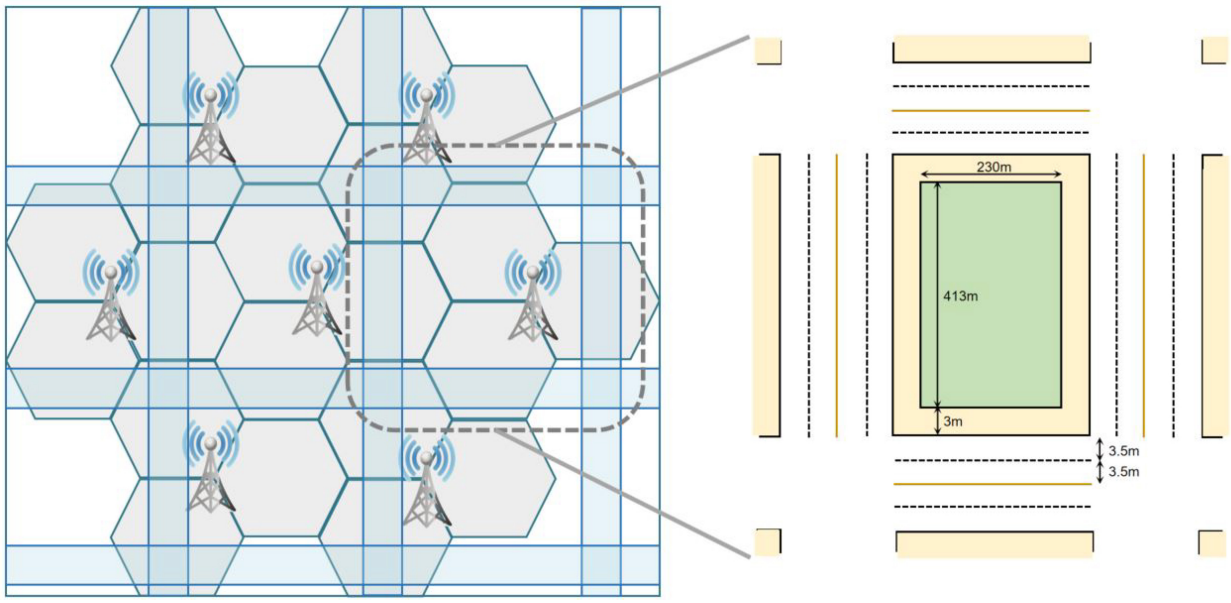

Fig. 6. Network layout for Outdoor–V2X–ISAC test environment.

velocity $\hat{v}_{\parallel,i}$. The radial velocity of the ST with respect to SensTRxP$_i$ can be written as

$$v_{\parallel,i} = v_x \sin\hat{\theta}_i \cos\hat{\phi}_i + v_y \sin\hat{\theta}_i \sin\hat{\phi}_i + v_z \cos\hat{\theta}_i \tag{28}$$

where $\hat{\theta}_i$ and $\hat{\phi}_i$ are, respectively, updated as $\theta_i = \arccos\left([\hat{z} - z_i]/\hat{d}_i\right)$ and $\hat{\phi}_i = \arctan\left([\hat{y} - y_i]/[\hat{x} - x_i]\right)$ with $\hat{d}_i = \sqrt{(\hat{x} - x_i)^2 + (\hat{y} - y_i)^2 + (\hat{z} - z_i)^2}$. Therefore, we can formulate the optimization problem as

$$\left(v_x, v_y, v_z\right) = \min_{v_x, v_y, v_z} \sum_{i=1}^{I} \varphi_i \left|\hat{v}_{\parallel,i} - v_{\parallel,i}\right| \tag{29}$$

where φ_i is the weighting coefficient. The optimization problem (29) can be solved again by using the interior-point method.

V. Test Environments and System Simulations

In this section, we present test environments, network layouts, evaluation configurations, and simulation platforms, which are important pieces of system simulations.

A. Test Environments and Network Layouts

Focusing on the key ISAC use cases as discussed in Section I which are V2X, UAV economy and smart manufacturing, we define three ISAC test environments.

1) *Outdoor–V2X–ISAC:* An urban environment with high-ST density focusing on vehicles. Regarding network layout, the base stations (BSs) or sites are placed in a regular grid, following a hexagonal layout with three TRxPs each, the same as the Dense Urban network layout in [16]. The STs are randomly dropped on the road lane as shown in Fig. 6, the same as the V2X network layout in [45].
2) *Outdoor–UAV–ISAC:* An urban environment with high-ST density focusing on UAVs. Regarding network layout, the BSs/sites are placed in a regular grid, following a hexagonal layout with three TRxPs each, the same as the Dense Urban network layout [16] as shown in Fig. 7. As Outdoor–V2X–ISAC and Outdoor–UAV–ISAC test environments both have dense-urban-style network layouts, we could merge these two into Dense Urban–ISAC test environments with different evaluation configurations.
3) *Indoor–Factory–ISAC:* An indoor isolated environment at factories focusing on automated guided vehicles (AGVs) with high-ST density. The BSs/sites are placed in 20-m spacing as shown in Fig. 8, with a floor surface of 120 m × 50 m containing 12 BSs/sites, which is the same as the indoor network layout in [16].

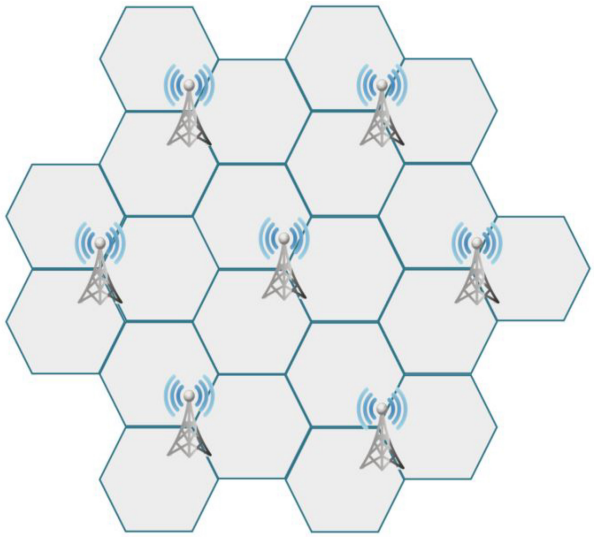

Fig. 7. Network layout for Outdoor–UAV–ISAC test environment.

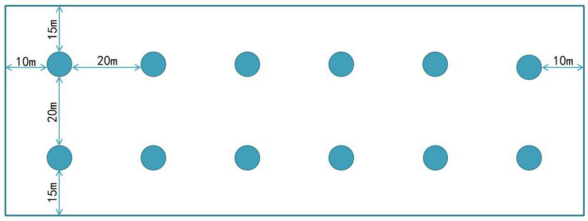

Fig. 8. Network layout for Indoor–Factory–ISAC test environment.

Simulation Procedure 1 Unified ISAC System Simulation

1: Configure simulation parameters and test environments.
2: Drop BS and initialize BS parameters.
3: Drop ST and UE, initialize corresponding parameters.
4: Generate sensing channel, communication channel and interference channel, respectively, include both large-scale and small-scale channels.
5: Perform ST-BS pairing and UE-BS pairing, respectively.
6: For a given slot, perform resource scheduling and signal transmission.
7: Update channel, SensTRxPs perform sensing signal reception and processing, CommTRxPs perform communication signal reception and processing.
8: Conduct slot loop of steps 6 and 7, and record simulation results for different targeted performance indicators.

Simulation Procedure 2 System-Level Simulation

1: Configure simulation parameters and test environments.
2: Drop BS and initialize BS parameters.
3: Drop ST and UE, initialize corresponding parameters.
4: Generate large-scale sensing channel, communication channel and interference channel, respectively.
5: Perform ST-BS pairing and UE-BS pairing, respectively.
6: For a given slot, perform resource scheduling.
7: Update channel, and calculate SINR.
8: Conduct slot loop of steps 6 and 7, and record SINR results.

B. Simulation Platforms

In this section, we give detailed procedures for system-level sensing simulation, link-level sensing simulation, and unified ISAC system simulation. The proposed unified ISAC system simulation is a platform that integrates both system-level and link-level sensing simulations, and is vital for KPI definition and evaluations of sensing capacity @sensing QoS. Detailed ISAC system simulation platform descriptions are shown in Simulation Procedure 1.

In addition, we also present system-level and link-level sensing simulation in Simulation Procedure 2 and 3, which is used for Evaluation Methodology 5 in Appendix B (detailed explanation of it will be presented in Section VI). The sensing system-level and link-level simulations are similar to those for communications, with sensing channel and sensing signal processing embedded. Given the absence of mature ISAC channel modeling, such system-level and link-level sensing simulations can reduce simulation workload, and are in nature very similar to the unified ISAC system simulation. Besides, the benefit of using system-level simulation plus link-level simulation is that we can obtain some intermediate results, such as SINR, to examine the sensing performance.

Simulation Procedure 3 Link-Level Simulation

1: Configure simulation parameters and test environments.
2: Drop BS and initialize BS parameters.
3: Drop ST and UE, initialize corresponding parameters.
4: Generate small-scale sensing channel, communication channel and interference channel, respectively.
5: Generate transmit signal, convolve with the small-scale channel.
6: Add interference and noise using the SINR results obtained from the system-level simulations to get the received signal.
7: Perform sensing signal processing, and record simulation results for different targeted performance indicators.

TABLE II
SIMULATION PARAMETERS FOR OUTDOOR-ISAC TEST ENVIRONMENTS

Parameters	Notation	Value
Center Frequency	f_c	7 GHz
Bandwidth	BW	100 MHz
Signal duration	T	20 ms
Subcarrier Spacing	SCS	60 kHz
Base station transmit power	P_t	52 dBm
Inter-site distance	ISD	200 m
Base station antenna height	h_{BS}	25 m
Number of vertical antennas	M	16
Number of horizontal antennas	N	8
Number of Polarization	P	2
Number of vertical channels	M_P	8
Number of horizontal channels	N_P	8
Antenna gain per element	G_{ant}	8 dBi
Antenna element vertical-spacing	d_{ant_v}	0.8λ
Antenna element horizontal-spacing	d_{ant_h}	0.5λ
Antenna electrical downtilt angle (V2X / UAV)	A_{dt}	11° / -11°
Radar cross section (V2X / UAV)	RCS	10 m^2 / 0.1 m^2
Sensing target height (V2X / UAV)	H_{ST}	0 m / 25 - 100 m

C. Evaluation Configurations

Detailed evaluation configurations and simulation parameters are given in Tables II and III. In the simulation, we focus on sensing processing where the sensing and communication functionalities operate at a time-division mode. We choose time-division mode because outstanding sensing localization performance requires a large bandwidth. Therefore, using time-division will provide more bandwidth and is also beneficial in terms of flexible signal scheduling. We use dedicated sensing reference signals in the simulation, and the Gold sequence is used for signal generation. Detailed sequence generation equation is not the focus of this article and relevant information can be found in [46].

As discussed in Section III-B, the sensing accuracy and resolution depend on time-frequency resources, and sensing accuracy can be perceived as plus and minus half of the resolution. Considering the localization resolution of $c/2B$, we

TABLE III
SIMULATION PARAMETERS FOR INDOOR-ISAC TEST ENVIRONMENTS

Parameters	Notation	Value
Center Frequency	f_c	26 GHz
Bandwidth	BW	400 MHz
Signal duration	T	10 ms
Subcarrier Spacing	SCS	120 kHz
Base station transmit power	P_t	24 dBm
Inter-site distance	ISD	20 m
Base station antenna height	h_{BS}	3 m
Number of vertical antennas	M	16
Number of horizontal antennas	N	8
Number of Polarization	P	2
Number of vertical channels	M_P	8
Number of horizontal channels	N_P	8
Antenna gain per element	G_{ant}	5 dBi
Antenna element vertical-spacing	d_{ant_v}	0.5λ
Antenna element horizontal-spacing	d_{ant_h}	0.5λ
Antenna electrical downtilt angle	A_{dt}	90°
Radar cross section (AGV)	RCS	1 m^2
Sensing target height (AGV)	H_{ST}	0 m

use 100 and 400 MHz, which will yield localization resolution of 1.5 and 0.375 m for outdoor and indoor configurations, respectively. Regarding velocity resolution of $\lambda/2T$, we use 20 and 10 ms, which will yield velocity resolution of 1.07 and 0.58 m for outdoor and indoor configurations, respectively.

It should be noted that as mentioned in Section V-B, system-level plus link-level simulations are conducted. Besides, the channel coefficient generation procedure is shown in Appendix A.

VI. SIMULATION RESULTS AND ANALYSIS

This section presents the simulation results of SensCAP. For sensing capacity simulations, as illustrated in Section V-B, since ISAC channel model is still under research, we use system-level plus link-level sensing simulations to reduce the simulation workload. The alternative Evaluation Methodology 5 in Appendix B is used in the simulation. This is in nature very similar to Evaluation Methodology 3, only with the ST dropping method changed (refer to Appendix B for more details). Also, another advantage of using system-level simulation plus link-level simulation is that we can obtain some intermediate results, such as SINR, to investigate the sensing performance more closely.

Regarding the sensing resource utilization, as shown in Tables II and III, the sensing signal duration is 20 and 10 ms for Outdoor-ISAC test environments and Indoor-ISAC test environments, therefore, the sensing resource utilization is only 2% and 1%, respectively. Such sensing resource utilization demonstrates the outstanding ISAC performance for both sensing and communication.

A. Sensing Probability

This section presents the simulation results of sensing probability. Table IV demonstrates the sensing detection probability given different false alarm rates. It can be observed that the sensing detection probability and false alarm rate hold a tradeoff, where the improvement of one will degrade the performance of the other one. This is because a larger false alarm rate indicates that the detection threshold has become lower, and a lower threshold leads to more targets detected, which results in an increased detection probability.

TABLE IV
SIMULATION RESULTS OF SENSING PROBABILITY

False Alarm Rate	Test Environments	Total number of dropped STs	Number of successfully detected STs	Detection Probability
10^{-3}	Outdoor - V2X - ISAC	11040	11040	100%
	Outdoor - UAV - ISAC	10500	10500	100%
	Indoor - Factory - ISAC	9396	9396	100%
10^{-4}	Outdoor - V2X - ISAC	11040	11010	99.73%
	Outdoor - UAV - ISAC	10500	10495	99.95%
	Indoor - Factory - ISAC	9396	9396	100%
10^{-5}	Outdoor - V2X - ISAC	11040	10890	98.64%
	Outdoor - UAV - ISAC	10500	10361	98.68%
	Indoor - Factory - ISAC	9396	9396	100%
10^{-6}	Outdoor - V2X - ISAC	11040	10410	94.29%
	Outdoor - UAV - ISAC	10500	9953	94.79%
	Indoor - Factory - ISAC	9396	9392	99.96%
10^{-7}	Outdoor - V2X - ISAC	11040	9390	85.05%
	Outdoor - UAV - ISAC	10500	9227	87.88%
	Indoor - Factory - ISAC	9396	9301	99.03%
10^{-8}	Outdoor - V2X - ISAC	11040	8640	78.26%
	Outdoor - UAV - ISAC	10500	8353	79.55%
	Indoor - Factory - ISAC	9396	8993	95.71%
10^{-9}	Outdoor - V2X - ISAC	11040	7740	70.11%
	Outdoor - UAV - ISAC	10500	7477	71.21%
	Indoor - Factory - ISAC	9396	8434	89.76%

B. Sensing Accuracy

This section presents the simulation results of sensing accuracy. Figs. 9–11 demonstrate the CDF curves of sensing localization error and velocity error for different test environments. Take the confidence level of 90% for localization and 70% for velocity, the localization accuracy is 1.44, 2.03, and 1.23 m and the velocity accuracy is 1.55, 4.46, and 0.95 m/s for Outdoor–V2X–ISAC test environment, Outdoor–UAV–ISAC test environment and Indoor–Factory–ISAC test environment, respectively. To get roughly 1 m or 1-m/s sensing accuracy, the confidence level we choose for velocity accuracy (70%) is lower than that of localization accuracy (90%). If we also choose 90% for the confidence level of velocity accuracy, for example in the V2X case, this will lead to 3-m/s velocity accuracy. This is because the velocity is estimated using Doppler estimation results from multiple SensTRxPs,

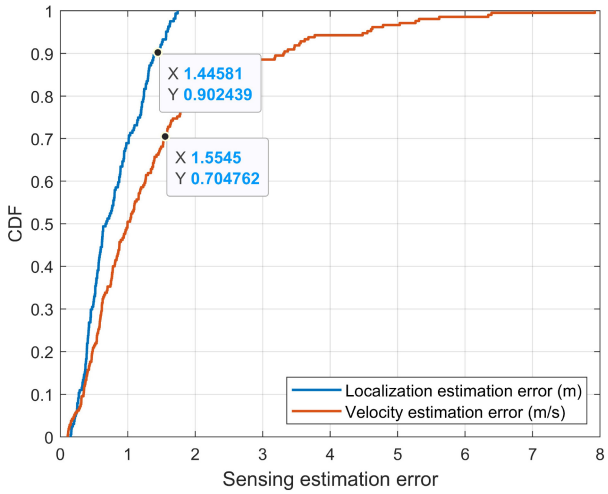

Fig. 9. Simulation results of sensing accuracy for Outdoor–V2X–ISAC test environment.

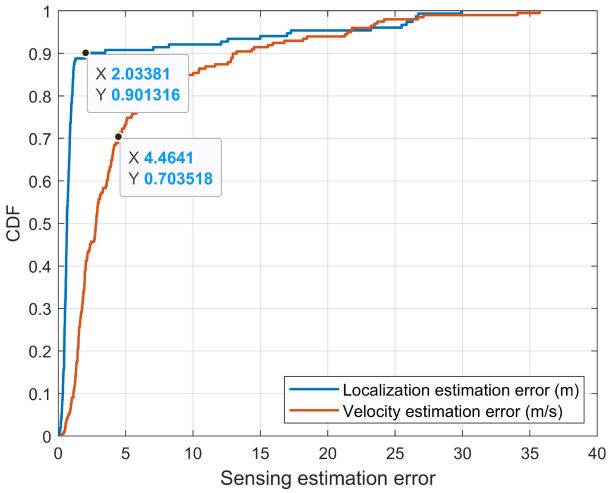

Fig. 10. Simulation results of sensing accuracy for Outdoor–UAV–ISAC test environment.

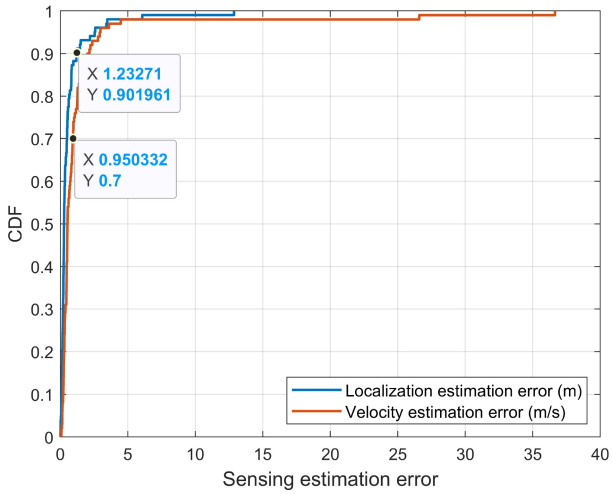

Fig. 11. Simulation results of sensing accuracy for Indoor–Factory–ISAC test environment.

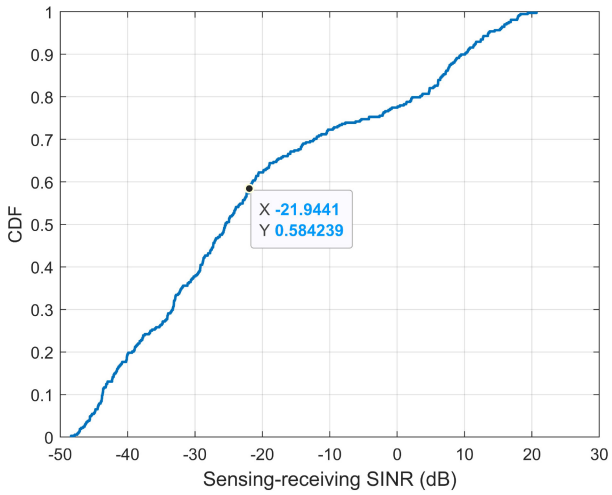

Fig. 12. Simulation results of sensing SINR that meets sensing QoS requirements when evaluating sensing capacity, given Outdoor–V2X–ISAC test environment.

one SensTRxP will yield the best SINR as well as sensing estimation performances, and the other SensTRxPs will have worse performance than the best one. Therefore, the velocity performance is degraded when using multiple SensTRxPs for velocity estimation. As mentioned in Section II-B, another method is to calculate average velocity using the location difference of two time-instances divided by the elapsed time. This should improve velocity estimation performance as only one SensTRxP with the best SINR is used for estimation. More simulations and corresponding analyses of such methods could be done in the future.

C. Sensing Capacity

This section presents the simulation results of sensing capacity. Figs. 12–14 demonstrate the simulation result of sensing SINR that meets sensing QoS requirements when evaluating sensing capacity, for Outdoor–V2X–ISAC test environment, Outdoor–UAV–ISAC test environment and Indoor–Factory–ISAC test environment, respectively. Figs. 15–16 show the simulation result of the relationship between sensing accuracy and SINR for Outdoor–ISAC and Indoor–ISAC test environments, respectively.

From the figures, we can find the relationship between SINR and sensing accuracy, and also the SINR threshold that meets sensing QoS. The STs are dropped as many as possible considering the physical environments and the localization resolution (refer to Appendix B for more details). Based on the link-level simulation results (Figs. 15 and 16), we can get the SINR that corresponds to sensing QoS requirements. By using this SINR as the threshold to analyze the CDF plots of system-level simulation results (Figs. 12–14), we can get the percentage of targets $R\%$ that fulfil sensing QoS requirements. Then we can get the number of targets $N_c = N \times R\%$ that fulfil sensing QoS requirements, and obtain sensing capacity $C = N_c/A$ accordingly, where N is the total number of dropped STs and A is the SensTRxP area. From the simulation results in this section, we can get the sensing capacity as shown in Table V.

TABLE V
SIMULATION RESULTS OF SENSING CAPACITY

Test Environments	Total number of dropped STs (N)	Number of successfully detected STs	Sensing Probability	Percentage of STs that meet Sensing QoS requirements ($R\%$)	Number of targets that meet Sensing QoS requirements ($N_c = N \times R\%$)	Area (A, in km^2)	Sensing Capacity ($C = N_c/A$)
Outdoor - V2X - ISAC	368	351	95.39% @ 10^{-6} false alarm	42%	155	0.2425	639 per km^2
Outdoor - UAV - ISAC	2100	1997	95.01% @ 10^{-6} false alarm	29%	609	0.2425	2511 per km^2
Indoor - Factory - ISAC	3132	3131	99.97% @ 10^{-6} false alarm	87%	2725	0.006	454167 per km^2

TABLE VI
SUGGESTED KPI VALUES FOR SENSCAP

Technical Performance Requirements	Test Environments	Suggested KPIs
Sensing Capacity @ Sensing QoS (Sensing Accuracy of l_a m localization accuracy and v_a m/s velocity accuracy, Sensing Probability of P_d detection probability and R_{fa} false alarm rate)	Outdoor - V2X - ISAC	600 per km^2 @ 1.5m localization accuracy @ 2m/s velocity accuracy @ 90% detection probability @ 10^{-6} false alarm rate
	Outdoor - UAV - ISAC	2500 per km^2 @ 2m localization accuracy @ 5m/s velocity accuracy @ 90% detection probability @ 10^{-6} false alarm rate
	Indoor - Factory - ISAC	400,000 per km^2 @ 1.25m localization accuracy @ 1 m/s velocity accuracy @ 95% detection probability @ 10^{-6} false alarm rate

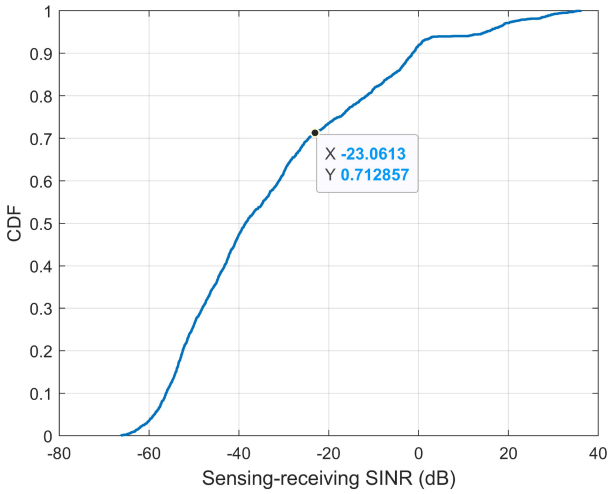

Fig. 13. Simulation results of sensing SINR that meets sensing QoS requirements when evaluating sensing capacity, given Outdoor–UAV–ISAC test environment.

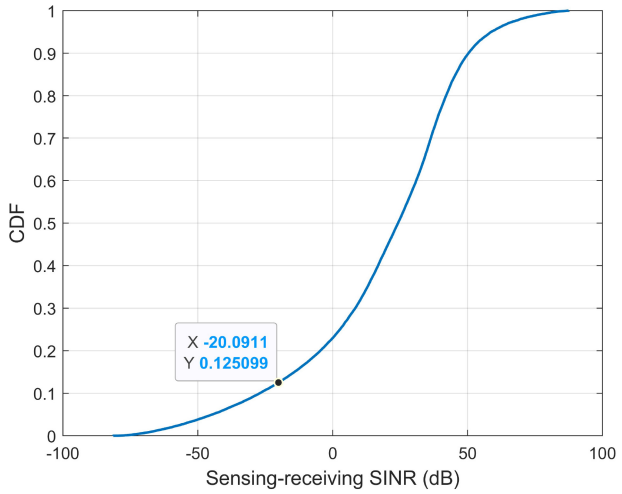

Fig. 14. Simulation result of sensing SINR that meets sensing QoS requirements when evaluating sensing capacity, given for Indoor–Factory–ISAC test environment.

VII. CONCLUSION

In summary, for the first time, we propose the technical performance requirement metric and corresponding evaluation methodologies for 6G ISAC to fill the gap in this area. Specifically, we propose SensCAP, a systematic sensing capability performance metric comprising sensing capacity, sensing accuracy, and sensing probability. The sensing probability and sensing accuracy build up sensing QoS, which is used to formulate sensing capacity. Sensing capacity reflects the comprehensive sensing performance, namely, the number of targets, that can be detected per unit area within unit time given sensing QoS requirements.

Furthermore, we illustrate evaluation methodologies, test environments, evaluation configurations, simulation platforms and simulation results for SensCAP. Based on the simulation results and analysis, Table VI gives the suggested values of SensCAP for different test environments. It's essential that the definition and evaluation methodologies of SensCAP can be used as a framework for the future standardization of ISAC. Different KPI values can be obtained given the research outcome on ISAC channel modeling and different simulation parameters, which will need more consensus in the industry.

Regarding future research direction, the definition and evaluation methodologies of SensCAP could be further improved by enriching the content of sensing QoS. For example, sensing air interface latency can also be part of sensing QoS, which sets

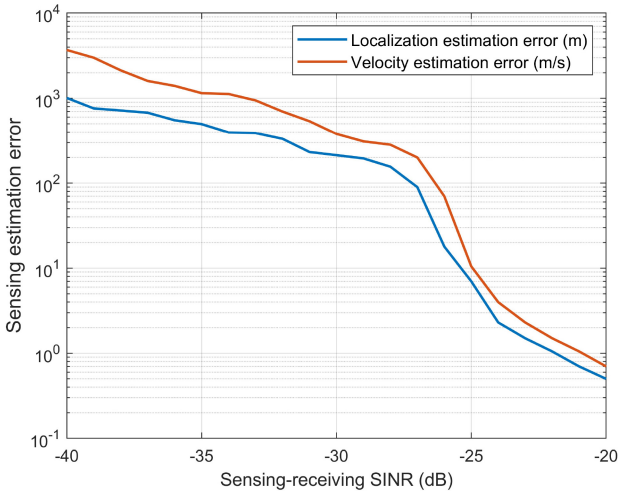

Fig. 15. Simulation results of the relationship between sensing accuracy and SINR for Outdoor–ISAC test environments.

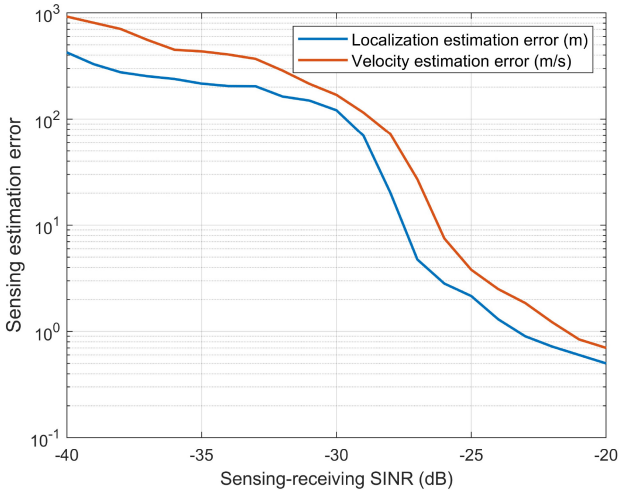

Fig. 16. Simulation results of the relationship between sensing accuracy and SINR for Indoor–ISAC test environment.

requirements on the time used to transmit the sensing signal. Then the definition of sensing capacity can be updated as the number of targets that can be detected per unit area given sensing QoS requirements which include sensing probability, accuracy, air interface latency, etc. Such sensing air interface latency can be part of the evaluation configurations for simulations, which pose stricter requirements than sensing resource utilization discussed in Section II-C. Considering the 3GPP numerology, a typical value of sensing air interface latency could be one or multiple times of 10 ms which is the length of a single frame. In terms of test environments and simulation setups, more representative use cases can be further investigated. For example, Outdoor–Rural–ISAC which focuses on intrusion detection of hazardous objects on highways and railways, and Indoor–Smart Home–ISAC which concentrates on home automation and health monitoring. Besides, the channel modeling of ISAC which may contain different kinds of interference should be considered thoroughly in the system simulation platform in light of 3GPP progress. Different sensing modes, including BS or UE monostatic, BS-BS, or BS-UE multistatic, could also be incorporated in the simulations. Furthermore, updated KPI values given new test environments, simulation configurations and mature ISAC channel model are essential and need to be further investigated in the future.

Evaluation Methodology 5 Alternative Evaluation Methodology for Sensing Capacity

1: Perform system-level simulation using the evaluation parameters for ISAC test environments in Tables II and III, and record the receive-end SINR for each ST. The total number of STs is N, where the intertarget distance relates to resolution.
2: Perform link-level simulation, generate sensing transmit signal, and obtain sensing receive signal for each target through the sensing channel information which consists of ST's true location and velocity as well as SINR obtained in step 1.
3: Record whether a target is present or not for a given false alarm rate R_{fa}, and calculate the detection probability P_{d_result}, which should be better than sensing probability performance requirements P_d.
4: Calculate the localization estimation error Δr and velocity estimation error Δv for each ST detected. Plot the CDF curves of Δr and Δv (or plot CDF of SINR obtained in step 1), and derive the percentage $R\%$ that fulfils both localization accuracy and velocity accuracy requirements.
5: Calculate the number of targets $N_c = N \times R\%$ that meet sensing QoS requirements. Then calculate the sensing capacity as $C = N_c/A$, where A is the SensTRxP area.

Appendix A
Channel Coefficient Generation

The detailed sensing channel coefficient generation procedure is shown in Fig. 17, which refers to [47] as the baseline. It should be noted that such channel generation mechanisms might be updated in light of the latest 3GPP discussions.

Appendix B
Alternative Evaluation Methodology for Sensing Capacity

The alternative evaluation methodology for sensing capacity is given in Evaluation Methodology 5. As mentioned in Section V-B, since ISAC channel model is still under research, we use system-level plus link-level sensing simulations to reduce the simulation workload. The alternative Evaluation Methodology 5 is in nature very similar to Evaluation Methodology 3, only with ST dropping method changed. Here, the STs are dropped considering the physical environments and the resolution, where the intertarget distance is localization resolution. The resolution is predefined using equation $c/2B$ or utilizing the outcome of the resolution simulation, where c is the speed of light and B is the sensing signal bandwidth. The target-dropping methods for different ISAC test environments are given as follows.

1) *Outdoor–V2X–ISAC:* Drop vehicles on each road lane considering road configuration for urban grid as shown

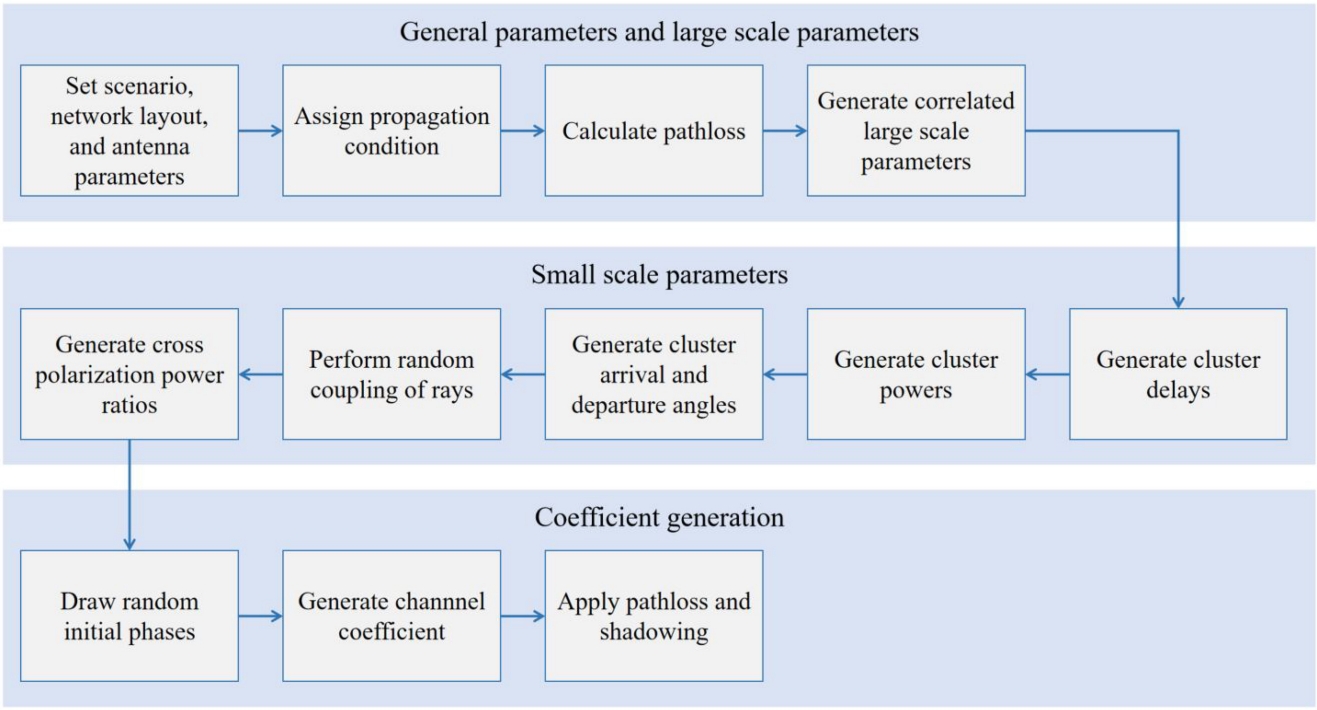

Fig. 17. Channel coefficient generation procedure.

in Fig. 6, assuming the length of a vehicle is 5m and intervehicle distance is 10m. The total number of vehicles is N.

2) *Outdoor–UAV–ISAC:* Drop $N_0 = 100$ UAVs per SensTRxP, which consists of $N_{\text{Cluster}} = 4$ UAV clusters, each cluster with $K = 25$ UAVs (x-axis with five UAVs multiple y-axis with five UAVs on a 2-D plane), the intertarget distance for any two UAVs along the x or y axes is localization resolution, $N_0 = N_{\text{Cluster}} \times K$. The UAV clusters are randomly distributed with heights shown in Table II. The total number of UAVs is $N = N_{TRxP} \times N_0$, where N_{TRxP} is the number of SensTRxP involved in the simulation.
3) *Indoor–Factory–ISAC:* Drop AGVs with a total number of N. The intertarget distance for any two AGVs along the x or y axes is the localization resolution, and assuming the AGV size is 1m × 1m.

The above ST dropping method is given as an example, which will lead to a total of N dropped targets. Through simulation, we can get $R\%$ of the total N targets that meet the sensing QoS requirements, hence the sensing capacity is obtained.

ACKNOWLEDGMENT

The authors would like to thank the 6G team members within the Future Research Lab at the China Mobile Research Institute, particularly Chunfeng Cui, Yajuan Wang, Xiaozhou Zhang, Zhitian Cheng, Zhiwen Sun, Siying Lv, Songhui Shen, and Xin Gui.

REFERENCES

[1] D. C. Nguyen et al., "6G Internet of Things: A comprehensive survey," *IEEE Internet Things J.*, vol. 9, no. 1, pp. 359–383, Jan. 2022.
[2] Y. Cui, F. Liu, X. Jing, and J. Mu, "Integrating sensing and communications for ubiquitous IoT: Applications, trends, and challenges," *IEEE Netw.*, vol. 35, no. 5, pp. 158–167, Sep./Oct. 2021.
[3] Y. Zhou et al., "Service aware 6G: An intelligent and open network based on convergence of communication, computing and caching," *Digit. Commun. Netw.*, vol. 6, no. 3, pp. 253–260, 2020.
[4] G. Liu et al., "Vision, requirements and network architecture of 6G mobile network beyond 2030," *China Commun.*, vol. 17, no. 9, pp. 92–104, Sep. 2020.
[5] Y. Qi, Y. Zhou, Y.-F. Liu, L. Liu, and Z. Pan, "Traffic-aware task offloading based on convergence of communication and sensing in vehicular edge computing," *IEEE Internet Things J.*, vol. 8, no. 24, pp. 17762–17777, Dec. 2021.
[6] Y. Peng et al., "How to tame mobility in federated learning over mobile networks?" *IEEE Trans. Wireless Commun.*, vol. 22, no. 12, pp. 9640–9657, Dec. 2023.
[7] G. Liu et al., "Cooperative sensing for 6G mobile cellular networks: Feasibility, performance and field trial," *IEEE J. Sel. Areas Commun.*, early access, Jun. 14, 2024, doi: 10.1109/JSAC.2024.3414596.
[8] Z. Wei et al., "Integrated sensing and communication signals toward 5G-A and 6G: A survey," *IEEE Internet Things J.*, vol. 10, no. 13, pp. 11068–11092, Jul. 2023.
[9] F. Liu, C. Masouros, A. P. Petropulu, H. Griffiths, and L. Hanzo, "Joint radar and communication design: Applications, state-of-the-art, and the road ahead," *IEEE Trans. Commun.*, vol. 68, no. 6, pp. 3834–3862, Jun. 2020.
[10] J. A. Zhang et al., "An overview of signal processing techniques for joint communication and radar sensing," *IEEE J. Sel. Topics Signal Process.*, vol. 15, no. 6, pp. 1295–1315, Nov. 2021.
[11] L. Ma, C. Pan, Q. Wang, M. Lou, Y. Wang, and T. Jiang, "A downlink pilot based signal processing method for integrated sensing and communication towards 6G," in *Proc. IEEE 95th Veh. Technol. Conf.*, 2022, pp. 1–5.
[12] L. Han et al., "Performance trade-off for a novel integrated Localization and communication system," in *Proc. IEEE 97th Veh. Technol. Conf.*, 2023, pp. 1–7.
[13] *Framework and Overall Objectives of the Future Development of IMT for 2030 and Beyond*, ITU-Rec. M.2160, Int. Telecommun. Union, Geneva, Switzerland, 2023.
[14] "IMT towards 2030 and beyond," Int. Telecommun.Union, Geneva, Switzerland, ITU-R 5D Document/1361, 2024. [Online]. Available:https://www.itu.int/md/R19-WP5D-C-1361/en

[15] "Minimum requirements related to technical performance for IMT-2020 radio interface(s)," Int. Telecommun. Union, Geneva, Switzerland, ITU-Rep. M.2410, 2017.
[16] "Guidelines for evaluation of radio interface technologies for IMT-2020," Int. Telecommun. Union, Geneva, Switzerland, ITU-Rep. M.2412, 2017.
[17] "Feasibility study on integrated sensing and communication," 3GPP, Sophia Antipolis, France, Rep. 22.837, 2023.
[18] "New SID: Study on channel modelling for integrated sensing and communication (ISAC) for NR," 3GPP, Edinburgh, U.K., Nokia, Espoo, Finland, document TSG RAN Meeting #102, 3GPP RP-234069, 2023.
[19] "RAN Chair: Summary for RAN Rel-19 package: RAN1/2/3-led," 3GPP Edinburgh, U.K., document TSG RAN Meeting #102, 3GPP RP-232745, 2023.
[20] "Discussion on channel modeling methodology for ISAC," 3GPP, Athens, Greece, China Mobile Commun. Group Co., Ltd., Beijing, China, Beijing Univ. Posts Telecommun., Beijing, China, Southeast Univ., Nanjing, China, Purple Mountain Lab, Nanjing, China, document TSG RAN WG1 Meeting #116, 3GPP R1-2400342, 2024.
[21] Z. Chai et al., "Empirical path loss channel modeling at 28 GHz for integrated sensing and communication system," in *Proc. Int. Conf. Wireless Commun. Signal Process. (WCSP)*, 2023, pp. 366–370.
[22] J. Wang, J. Zhang, Y. Zhang, T. Jiang, L. Yu, and G. Liu, "Empirical analysis of sensing channel characteristics and environment effects at 28 GHz," in *Proc. IEEE Globecom Workshops (GC Wkshps)*, 2022, pp. 1323–1328.
[23] J. Zhang et al., "Integrated sensing and communication channel: Measurements, characteristics, and modeling," *IEEE Commun. Mag.*, vol. 62, no. 6, pp. 98–104, Jun. 2024.
[24] J. Zhang et al., "Channel measurement, modeling, and simulation for 6G: A survey and tutorial," 2023, *arXiv:2305.16616*.
[25] "Discussion on ISAC channel model," 3GPP, Athens, Greece, Xiaomi Inc., Beijing, China, Beijing Univ. Posts Telecommun., Beijing, China, document TSG RAN WG1 Meeting #116, 3GPP R1-2400573, 2024.
[26] "Views on Rel-19 ISAC channel modeling," 3GPP, Athens, Greece, Sweden, Vivo, Dongguan, China, document TSG RAN WG1 Meeting #116, 3GPP R1-2400257, 2024.
[27] Y. Liu, J. Zhang, Y. Zhang, Z. Yuan, and G. Liu, "A shared cluster-based stochastic channel model for integrated sensing and communication systems," *IEEE Trans. Veh. Technol.*, vol. 73, no. 5, pp. 6032–6044, May 2024.
[28] Y. Liu, J. Zhang, Y. Zhang, H. Gong, T. Jiang, and G. Liu, "How to extend 3D GBSM to integrated sensing and communication channel with sharing feature?" *IEEE Wireless Commun. Lett.*, early access, May 7, 2024, doi: 10.1109/LWC.2024.3397839.
[29] M. I. Skolnik, *Introduction to Radar Systems*, 3rd ed. New York, NY, USA: McGraw-Hill, 2001.
[30] M. A. Richards, *Fundamentals of Radar Signal Processing*. New York, NY, USA: McGraw-Hill Educ., 2014.
[31] L. Xiao, Y. Liu, T. Huang, X. Liu, and X. Wang, "Distributed target detection with partial observation," *IEEE Trans. Signal Process.*, vol. 66, no. 6, pp. 1551–1565, Mar. 2018.
[32] J. Chen et al., "A sparsity based CFAR algorithm for dense radar targets," in *Proc. IEEE Radar Conf.*, 2020, pp. 1–6.
[33] "Study on NR positioning support," 3GPP, Sophia Antipolis, France, Rep. 38.855, 2019.
[34] S. M. Kay, *Fundamentals of Statistical Signal Processing*. Hoboken, NY, USA: Prentice Hall, 1993.
[35] A. Shahmansoori, G. E. Garcia, G. Destino, G. Seco-Granados, and H. Wymeersch, "Position and orientation estimation through Millimeter-wave MIMO in 5G systems," *IEEE Trans. Wireless Commun.*, vol. 17, no. 3, pp. 1822–1835, Mar. 2018.
[36] A. Sakhnini, M. Guenach, A. Bourdoux, and S. Pollin, "A Cramér–Rao lower bound for analyzing the localization performance of a multistatic joint radar-communication system," in *Proc. 1st IEEE Int. Online Symp. Joint Commun. Sens.*, 2021, pp. 1–5.
[37] Z. Wei et al., "5G PRS-based sensing: A sensing reference signal approach for joint sensing and communication system," *IEEE Trans. Veh. Technol.*, vol. 72, no. 3, pp. 3250–3263, Mar. 2023.
[38] A. Liu et al., "A survey on fundamental limits of integrated sensing and communication," *IEEE Commun. Surveys Tuts.*, vol. 24, no. 2, pp. 994–1034, 2nd Quart., 2022.
[39] "Guidelines for evaluation of radio interface technologies for IMT-advanced," Int. Telecommun. Union, Geneva, Switzerland, ITU-Rep. M.2135, 2009.
[40] Q. Shi, L. Liu, and S. Zhang, "Joint data association, NLOS mitigation, and clutter suppression for networked device-free sensing in 6G cellular network," in *Proc. IEEE Int. Conf. Acoust., Speech Signal Process. (ICASSP)*, 2023, pp. 1–5.
[41] X. Wang et al., "Multipath-exploited bistatic sensing with LoS blockage in MIMO-OFDM systems for 6G," in *Proc. IEEE Int. Conf. Commun. Workshops (ICC Workshops)*, to be published.
[42] W. Yang et al., "Integrated sensing and communication channel modeling and measurements: Requirements and methodologies toward 6G Standardization," *IEEE Veh. Technol. Mag.*, vol. 19, no. 2, pp. 22–30, Jun. 2024.
[43] C. Sturm and W. Wiesbeck, "Waveform design and signal processing aspects for fusion of wireless communications and radar sensing," *Proc. IEEE*, vol. 99, no. 7, pp. 1236–1259, Jul. 2011.
[44] Z. Han et al., "Multistatic integrated sensing and communication system in cellular networks," in *Proc. IEEE Globecom Workshops (GC Wkshps)*, 2023, pp. 123–128.
[45] "Study on evaluation methodology of new vehicle-to-everything (V2X) use cases for LTE and NR," 3GPP, Sophia Antipolis, France, Rep. 37.885, 2018.
[46] *NR Physical Channels and Modulation*, 3GPP Standard TS 38.211, 2023.
[47] "Study on channel model for frequencies from 0.5 to 100 GHz," 3GPP, Sophia Antipolis, France, Rep. 38.901, 2019.

Guangyi Liu received the Ph.D. degree from Beijing University of Posts and Telecommunications, Beijing, China, in 2006.

He is currently the Chief Scientist of 6G in China Mobile Communication Corporation (CMCC), the Founding Member and the Co-Chair of the 6G Alliance of Network AI, and the Vice-Chair of the THz Industry Alliance in China and the Wireless Technology Working Group of IMT-2030 (6G) Promotion Group supported by Ministry of Information and Industry Technology of China. He has been leading the 6G Research and Development with CMCC since 2018. He has led the Research and Development of 4G's evolution and 5G in CMCC from 2006 to 2020. He has acted as a Spectrum Working Group Chair and the Project Coordinator of LTE Evolution and 5G eMBB in Global TD-LTE Initiative from 2013 to 2020 and led the industrialization and globalization of TD-LTE evolution and 5G eMBB.

Liang Ma received the B.Eng. degree in electrical and electronic engineering from the University College London, London, U.K., in 2018, and the M.Sc. degree in communications and signal processing from Imperial College London, London, in 2019.

He has been with Future Research Lab, China Mobile Research Institute, Beijing, China, since 2020. He is a member of the Chinese Delegation to ITU-R, and is also involved in the work of other standardization organizations, including 3GPP and NGMN, internationally, as well as IMT-2030 (6G) Promotion Group and CCSA, domestically. His research interests include 6G, integrated sensing and communication, MIMO, nonorthogonal multiple access, and interference management.

Yahui Xue received the M.S. degree in geodetection and information technology from Central South University, Changsha, China, in 2020.

He has been with Future Research Lab, China Mobile Research Institute, Beijing, China, since 2020. His research interests include wireless communications, integrated sensing, and communication and multiple input multiple output systems.

Lincong Han received the B.S. degree in communication engineering from Shandong University, Jinan, China, in 2017, and the Ph.D. degree in communication and information systems from Beihang University, Beijing, China, in 2023.

She has been with Future Research Lab, China Mobile Research Institute, Beijing, since 2023. Her research interests include 6G, integrated sensing and communication, and MIMO and interference management.

Rongyan Xi received the B.S. degree in communication engineering from Shandong University, Jinan, China, in 2017, and the Ph.D. degree in electronic engineering from Tsinghua University, Beijing, China, in 2023.

She has been with Future Research Lab, China Mobile Research Institute, Beijing, since 2023. Her research interests include 6G, integrated sensing and communication, MIMO, target detection, and positioning and system design.

Zixiang Han (Member, IEEE) received the bachelor's degree in electronic science and technology from Nanjing University, Nanjing, China, in 2018, and the Ph.D. degree in electronic and computer engineering from The Hong Kong University of Science and Technology, Hong Kong, in 2022.

He is currently a Project Manager with the Future Research Lab, China Mobile Research Institute, Beijing, China. His current research interests include integrated sensing and communication, compact MIMO antennas, MIMO systems, antenna design, and optimization.

Hanning Wang received the Double B.S. degrees in information engineering from Beijing Institute of Technology, Beijing, China, and Australian National University, Canberra, ACT, Australia, in 2014, and the M.S. degree in electronics and telecommunications engineering from Australian National University in 2015.

She is a member of Technical Staff, Future Research Lab, China Mobile Research Institute, Beijing. Her current research interests include 6G, wireless communication, integrated sensing and communication, and MIMO.

Jing Dong received the M.S. degree in telecommunication engineering from Xidian University, Xi'an, China, in 2016.

She is currently with China Mobile Research Institute, Beijing, China. Her current research interests include 6G visions and requirements, integrated sensing and communication, and multidimensional integrated networking.

Mengting Lou received the B.S. and M.S. degrees from Beijing Jiaotong University, Beijing, China, in 2015 and 2019, respectively.

She is a member of Technical Staff, Future Research Lab, China Mobile Research Institute, Beijing. Her current research interests include wireless communications, integrated sensing and communication, virtual multi-input–multioutput, sparse array, and coordinated multipoint transmission.

Jing Jin received the B.S. and Ph.D. degrees from Beijing University of Posts and Telecommunications, Beijing, China, in 2006 and 2011, respectively.

She is a Principal Member of Technical Staff, Future Research Lab, China Mobile Research Institute, Beijing. Her research interests include wireless communications, MIMO, multiuser beamforming, and interference cancelation.

Qixing Wang received the B.S., M.S., and Ph.D. degrees in information and communication engineering from Beijing University of Posts and Telecommunications, Beijing, China, in 2002, 2005, and 2008, respectively.

He is a Principal Member of Technical Staff responsible for 6G in Future Research Lab, China Mobile Research Institute, Beijing. His research interests include wireless technology research and development, including 5G and 6G.

Yifei Yuan (Fellow, IEEE) received the bachelor's and master's degrees from Tsinghua University, Beijing, China, in 1993 and 1996, respectively, and the Ph.D. degree from Carnegie Mellon University, Pittsburgh, PA, USA, in 2000.

He was with Lucent Technologies Bell Labs, Murray Hill, NJ, USA, from 2000 to 2008. From 2008 to 2020, he was a Technical Director and a Chief Engineer with ZTE Corporation, Shenzhen, China, responsible for standards and research of LTE-Advanced and 5G. He has been the Chief Expert with China Mobile Research Institute, Beijing, since 2020, responsible for 6G. He has extensive publications, including 12 books on key air interface technologies of 4G, 5G, and 6G mobile communications. He has more than 60 granted U.S. patents.